

# Parametric Analysis of a Double E-shaped Meander Line Monopole Antenna for UHF Applications

N. Ripin, A. A. Sulaiman, N. E. Rashid, M. F. Hussin, and N. N. Ismail

**Abstract**—A compact double E-shaped meander line monopole antenna for Ultra High Frequency (UHF) applications is proposed. Aim of this study is to design a small and compact printed monopole antenna resonates at UHF band. By adding slots and meander line on the radiating patch, the resonant frequency of the antenna can be reduced with no significant effects on other antenna performances. With overall size of 83.80 mm x 143.74 mm corresponding to  $0.123 \lambda_0 \times 0.211 \lambda_0$ , the antenna resonant frequency is reduced from 878 MHz to 440 MHz by inserting the proposed method. Defected ground structure (DGS) is introduced on the partial ground plane to improve the reflection coefficient of the proposed antenna. Parametric analysis are conducted and investigated to provide good antenna performances at targeted frequency band. The proposed antenna exhibits an omnidirectional radiation pattern.

**Index Terms**—Printed monopole antenna, slots, meander line, UHF, miniaturization, omnidirectional radiation pattern,

## I. INTRODUCTION

IN selecting an antenna topology for omnidirectional UHF band applications, a number of aspects need to be considered including size, physical profile, compatibility, complexity, and radiation pattern. Typically, wire antennas such as dipole, monopole and whip antennas were used for omnidirectional UHF applications where the size of the antenna is relatively small compared to the wavelength. However, wire antennas are having difficulties in manufacturing using printed circuit techniques and incompatible with Monolithic Microwave Integrated Circuits (MMIC). Therefore, printed antennas are selected to replace the wire antennas especially for UHF applications. Nevertheless the printed antenna is not suitable for low frequency band due to the large size of the antenna. Hence, the size of the printed antenna has to be reduced.

Recently, various antenna miniaturization techniques have been studied and investigated. Mitra et. al miniaturize

CPW-fed ring slot antenna size using interdigitated slits [1]. The interdigitated slits-loaded structure reduces resonant frequency of the antenna. By loading multiple interdigitated slits inside the ring, further reduction in resonant frequency is achieved up to 54.46%.

As stated in [2], Wang et al. found that the size of CPW-fed antipodal Vivaldi antenna (AVA) can be reduced using elliptically shaped strip conductors. The strips conductors act as two arms of the antenna are capable in reducing the antenna operating frequency. The radiation performance of the antenna is improved using tapered slots on the antenna arms. The proposed antenna size of 90 x 93.5 x 0.8 mm<sup>3</sup> cover the impedance bandwidth from 1.32 GHz to 17 GHz. Nevertheless, the proposed structure is quite complicated and its overall size is relatively big compared to high operating wavelength.

Fujimoto et.al proposed a miniature printed monopole antenna using cutting method [3]. The printed rectangular monopole antenna is cut into trapezoidal form where half of the patch area that resides very weak electric current is removed. This technique has led to 53% antenna size miniaturization.

Mondal et al. showed that the shorting strip and meander line structure reduce the length of the planar rectangular metal antenna [4]. The meander line technique has reduced the size of the shorted planar rectangular metal antenna (SPRMA) by about 16% while the shorting strip has allowed the meander line antenna to be reduced by 40%. The proposed antenna were produced bi-directional radiation pattern.

Slot technique has been widely used in antenna design as reported in [5]–[11]. Slots are inserted on the patch of the antenna to increase the circumferences of the patch. Hence, the effective capacitance and effective inductance can be increased as well. This will lead to the decrement of the resonant frequency.

A meander line technique was employed in designing a compact printed monopole antenna for Long Term Evolution (LTE) mobile handset [12]. The meander line radiator is connected to the L-shaped radiator where the meander branch operates at lower band while the L-shaped branch operates at upper band. The radiator has a small size of 18 x 21 mm<sup>2</sup> but with the large ground plane that make whole antenna size to be 70 x 118 mm<sup>2</sup>. Unlike the ideal monopole antenna, the radiation pattern of the proposed antenna was restricted.

In this study, slots are combined with the meander line and

Submitted on 2<sup>nd</sup> March 2017 and accepted on 6<sup>th</sup> June 2017. This work was supported in part by the Universiti Teknologi MARA under Holistic Success Module code no. 600-IRMI/DANA 5/3/ARAS (0028/2016).

N. Ripin, A. A. Sulaiman, N. E. A. Rashid, M. F. Hussin and N. N. Ismail were with Applied Electromagnetic Research Group (AERG), Faculty of Electrical Engineering, Universiti Teknologi MARA, 40450 Shah Alam, Selangor, Malaysia (e-mail: nabilahripin@yahoo.com, asari100@salam.uitm.edu.my, emileen98@salam.uitm.edu.my, fahmi478@salam.uitm.edu.my, nornajwaismail88@gmail.com).

defected ground structure (DGS) to reduce the resonant frequency of the antenna. Similar to the slots, meander line is proposed to increase the effective capacitance and inductance of the radiator. Whereas the DGS is used to improve the reflection coefficient of the antenna. The novelty of this design is on the novel structure of double E-shaped connected through a meander line backed by a partial ground plane. The proposed antenna produces omnidirectional radiation pattern at UHF band. This study presents the simulation result only where the experimental verification will be completed in future work.

## II. ANTENNA DESIGN AND APPROACH

In this study, a square printed monopole antenna is designed as a reference antenna. Slots and meander line are introduced on the square radiating patch to increase the effective length of the radiator so that the resonant frequency would be reduced. All antennas were designed on FR-4 substrate with dielectric constant  $\epsilon_r = 4.3$ , substrate height  $h = 1.6$  mm and loss tangent of 0.025. The antenna is fed by a  $50\Omega$  microstrip line backed by partial ground plane. The radiating patch, feed line and the ground plane are made of copper with thickness of 0.035 mm. They have been simulated using Computer Simulation Technology (CST) Microwave Studio (MWS) software. All antenna parameters were optimized and analyzed using Genetic Algorithm (GA) optimizer to obtain the best performances of the antenna. The evolution of various antenna configurations are explained in *Section A*, *Section B*, *Section C*, *Section D* and *Section E*.

### A. Reference Antenna

The square shaped patch monopole antenna is designed as a reference antenna. The antenna consists of a square shaped patch with width,  $W_p$  of 74.20 mm and length,  $L_p$  of 74.20 mm connected to a  $50\Omega$  transmission line backed by a partial ground plane.  $W_f$  of 3 mm and  $L_f$  of 64.74 mm denote the width and the length of the feed line, respectively. The partial ground plane at the bottom layer of the antenna as depicted in Fig. 1 has width,  $W_g$  and length,  $L_g$  of 83.80 mm and 60 mm, respectively. In this study, the main objective of designing a partial ground plane is to produce omnidirectional radiation pattern at resonant frequency. Overall size of the antenna is represented by the size of the substrate with width,  $W_s$  of 83.80 mm and length,  $L_s$  of 143.74 mm.

A few calculations of the reference antenna's dimensions have been completed based on the guided wavelength in the dielectric substrate. Commonly, the length of the radiating patch is about one half of the guided wavelength corresponding to the operational frequency [13]–[15] which presented by:

$$L_p = \frac{\lambda_g}{2} \quad (1)$$

$$\lambda_g = \frac{\lambda_0}{\sqrt{\epsilon_r + 1}} \quad (2)$$

$$\lambda_0 = \frac{c}{f_r} \quad (3)$$

Where;  $\lambda_g$  is the guided wavelength,  $\lambda_0$  is free space wavelength,  $c$  is the speed of light ( $c = 3 \times 10^8$  m/s) and  $f_r$  is the resonant frequency. In this study, the targeted operating frequency band must cover 878 MHz.

The optimization process is done by varying one parameter at a time while others are fixed. For the reference antenna, the length of the ground plane,  $L_g$  is varied to observe the effect of the ground plane on the simulated reflection coefficient. Fig. 2 demonstrates the graph of different  $L_g$  on the simulated reflection coefficient. It is clearly observed that as the value of  $L_g$  increased, the reflection coefficient of the antenna decreased. Therefore, the optimum length of the ground plane should be 60 mm.

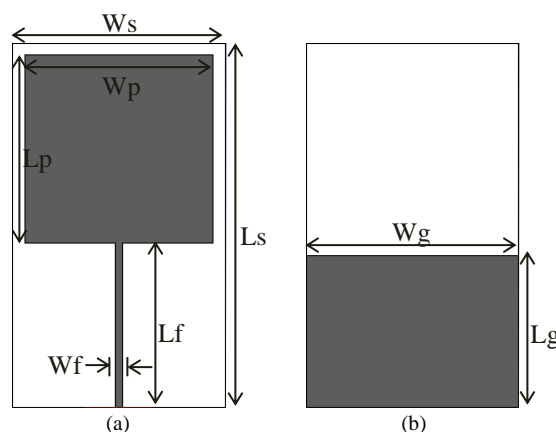


Fig. 1. Configuration of the reference antenna (a) front view (b) back view.

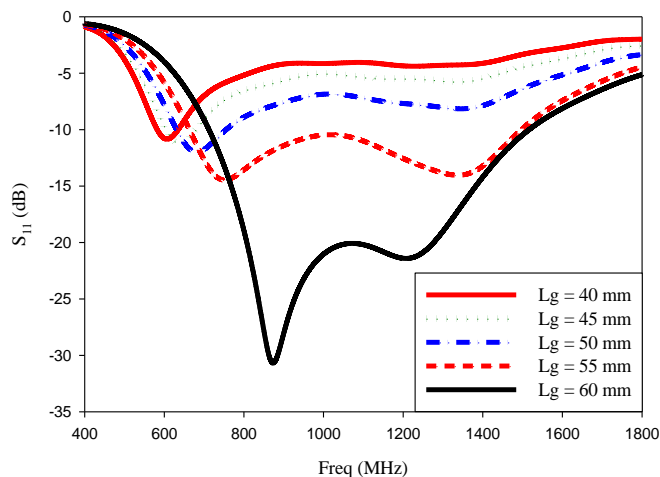


Fig. 2. Simulated reflection coefficient of various ground plane length  $L_g$ .

### B. I-shaped Patch Monopole Antenna

Slots are introduced on the right and left side of the radiator to lengthen its circumference. This will lead to the increment of the effective capacitance and inductance, hence reducing the resonant frequency of the antenna. Embedded slots on both sides of the patch resulting in an I-shaped patch configuration as displayed in Fig. 3. Each parameters of the I-shaped

antenna are similar to the reference antenna except for the additional square slot with width and length denoted by  $a$ .

The effect of various length and width of the slot on the simulated reflection coefficient is observed in Fig. 4. It is clearly seen that as  $a$  increases, the resonant frequency decreases. The value of  $a$  cannot be further increased because it could affect the value of thin line  $b$  as well. In this study, the width of the thin line,  $b$  cannot be made smaller than 1 mm to avoid difficulties in antenna fabrication process. From the result, it is clear that the antenna resonates at lowest frequency band when  $a$  is 36.6 mm.

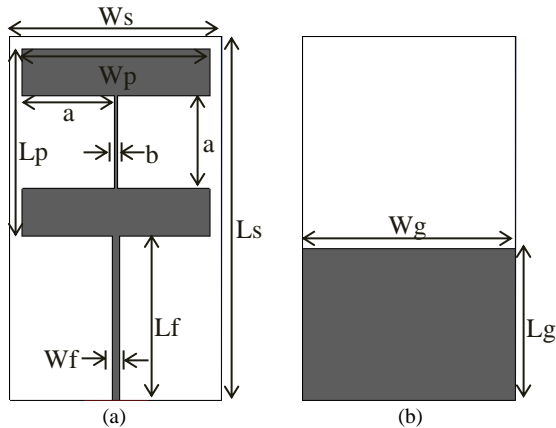


Fig. 3. Configuration of the I-shaped antenna (a) front view (b) back view.

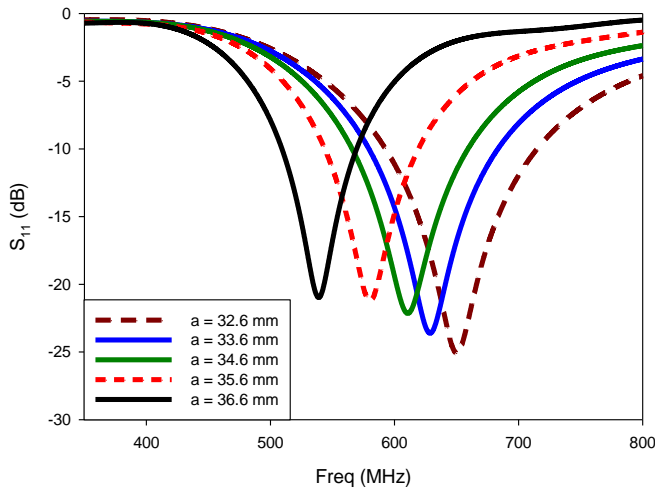


Fig. 4. Simulated reflection coefficient of various width / length of the slots  $a$ .

### C. Double E-shaped Patch Monopole Antenna

Another slots are introduced onto the I-shaped patch to further increase the length of the radiator so that the antenna resonant frequency can be further decreased. Similar to the I-shaped monopole patch antenna, the slots are constructed on the strongest current path on the patch. Four slots have been created on the upper and bottom layer of the patch as demonstrated in Fig. 5. The addition of the slots to the I-shaped monopole changing the patch structure from I-shaped to double E-shaped patch. All parameters are similar to the reference antenna except for additional slots on the patch. The added slots have a square shaped with width and length

denoted by  $w_l$  and  $l_l$ , respectively.

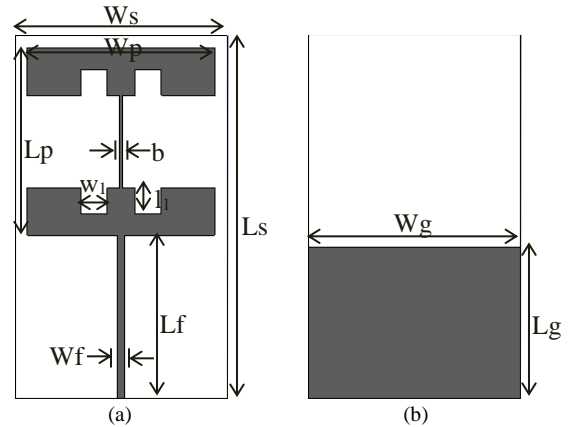


Fig. 5. Configuration of the double E-shaped antenna (a) front view (b) back view.

The width of the slot,  $w_l$  is varied as presented in Fig. 6. From the graph, the simulated reflection coefficient remain the same even for different values of  $w_l$ . Since the width of the slots has no effect on the simulated reflection coefficient, any value of  $w_l$  can be set for the slots. In this study,  $w_l$  is set at 10.3 mm.

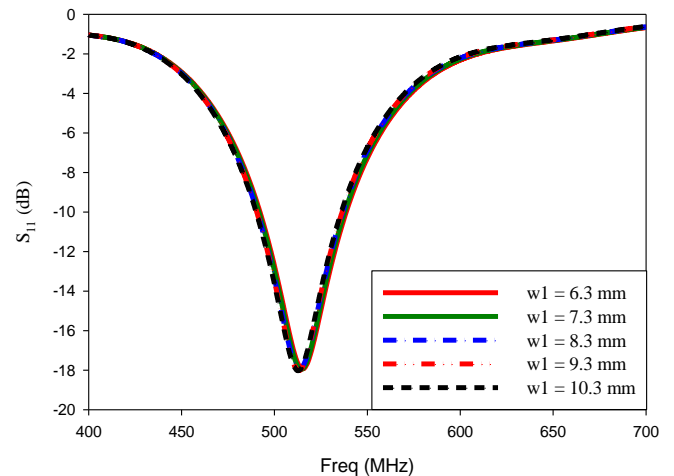


Fig. 6. Simulated reflection coefficient of various width of the slots  $w_l$ .

The length of the slots are also analysed to observe the effects of  $l_l$  on the simulated reflection coefficient as shown in Fig. 7. It is shown that the resonant frequency decreased as  $l_l$  increased. Therefore, the best value of  $l_l$  is chose to be 10.3 mm.

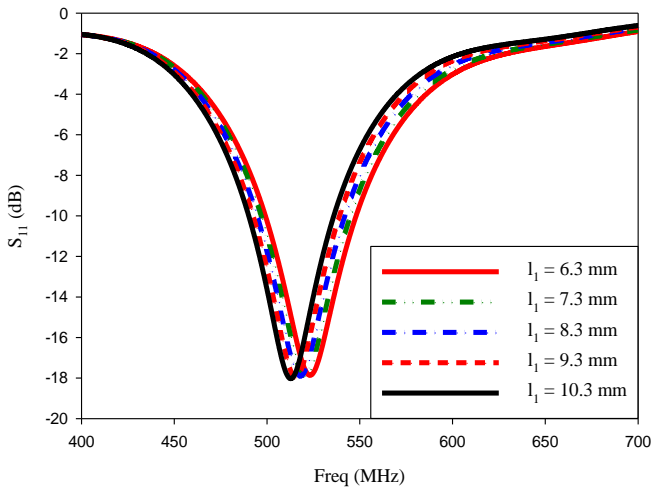


Fig. 7. Simulated reflection coefficient of various length of the slots  $l_1$ .

**D. Double E-shaped Meander Line Monopole Antenna**

The evolution of the antenna from reference antenna to the double E-shaped monopole antenna has achieved reduction in antenna resonant frequency of 366 MHz which is from 878 MHz to 512 MHz. The resonant frequency still need to be reduced in order to miniaturize the monopole antenna to be as small as possible. For that reason, the thin line that connects the double E-shaped patch is modified and replaced with the meander line. The configuration of the double E-shaped patch connected through a meander line is exposed in Fig. 8. Meanwhile, Fig. 9 shows the configuration of the meander line which consists of  $l_a = 5.27$  mm,  $w_a = 9.50$  mm,  $w_b = 18$  mm,  $w_c = 1.00$  mm,  $w_d = 5.12$  mm and  $w_e = 5.12$  mm.

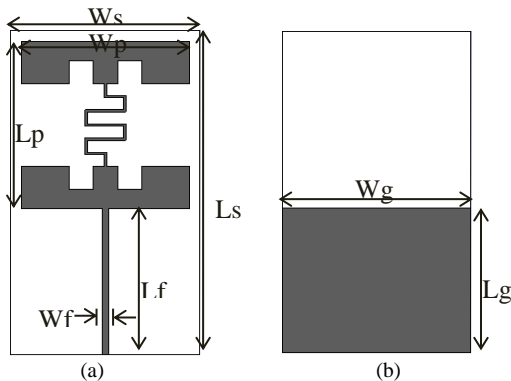


Fig. 8. Configuration of the double E-shaped meander line antenna (a) front view (b) back view.

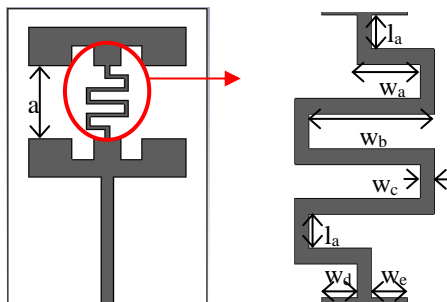


Fig. 9. Configuration of the radiator (meander line is enlarged for visibility).

The length of the ground plane of the double E-shaped patch connected through a meander line is optimized to improve the antenna reflection coefficient.  $L_g$  is varied as displayed in Fig. 10 where the graph shows that the reflection coefficient is optimum when the  $L_g$  is increased to 64.7 mm.

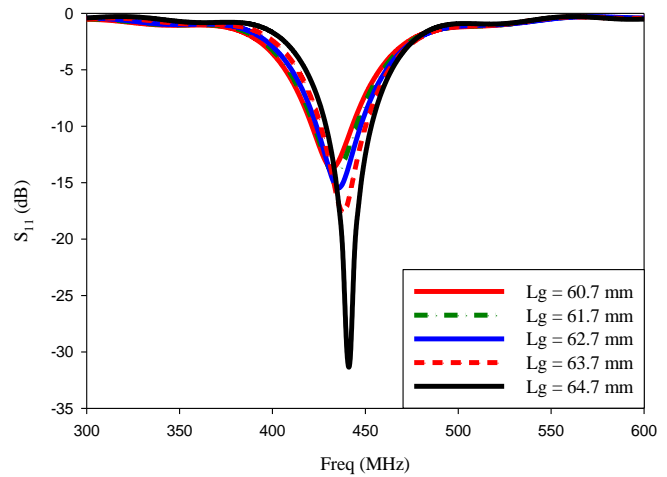


Fig. 10. Simulated reflection coefficient of various length of the slots  $L_g$ .

The insertion of meander line with optimized ground plane length lead to a reduction in antenna resonant frequency from 512 MHz to 442 MHz. Dimensions of meander line  $w_a$  and  $w_b$  are analysed to investigate the effect of various meander line width and length on the simulated reflection coefficient. Fig. 11 and Fig. 12 illustrate the effect of various  $w_a$  and  $w_b$  on the simulated reflection coefficient, respectively. The simulated reflection coefficient curve is at optimum level when  $w_a$  is 9.5 mm where the resonant frequency is at 442 MHz with reflection coefficient of -30.25 dB. While the ideal value of  $w_b$  is 18 mm.

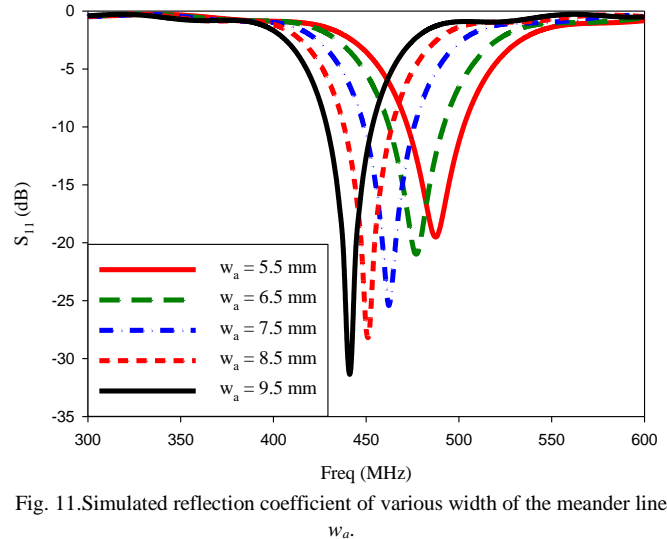


Fig. 11. Simulated reflection coefficient of various width of the meander line  $w_a$ .

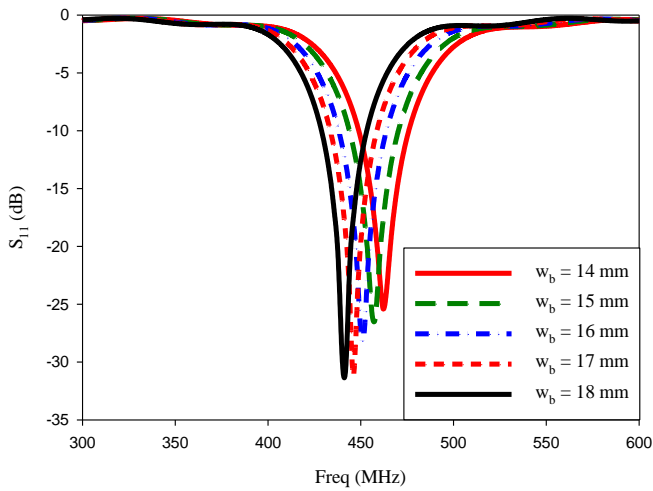


Fig. 12. Simulated reflection coefficient of various length of the meander line  $w_b$ .

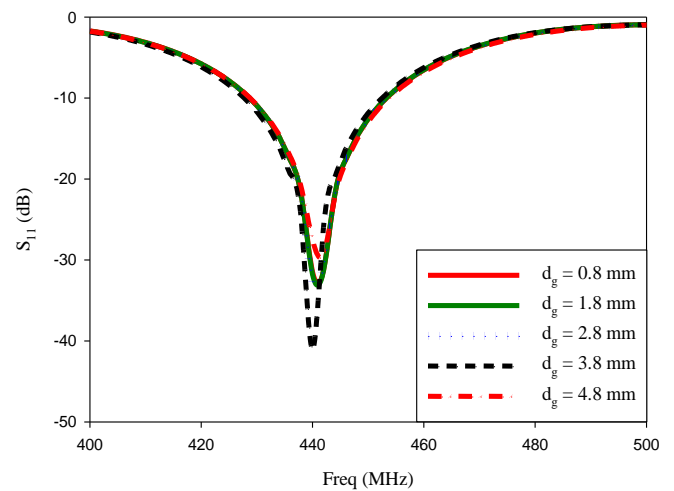


Fig. 14. Simulated reflection coefficient of various length of the DGS  $d_g$ .

### E. Double E-shaped Meander Line Monopole Antenna with DGS

Up till now, the resonant frequency has been reduced from 878 MHz to 442 MHz with a slight influence on the antenna reflection coefficient. However, the reflection coefficient of the antenna can be further improved to ensure that the antenna will radiate well even in a real testing. The reflection coefficient can be improved by inserting a slot or defected ground structure (DGS) on the ground plane as illustrated by Fig. 13.

The square DGS is varied to observe its effect on the simulated reflection coefficient as illustrated in Fig. 14. It is clearly shown that the optimal value of the length of DGS denoted by  $d_g$  is at 3.8 mm where the reflection coefficient is at minimum level with resonant frequency of 440 MHz.

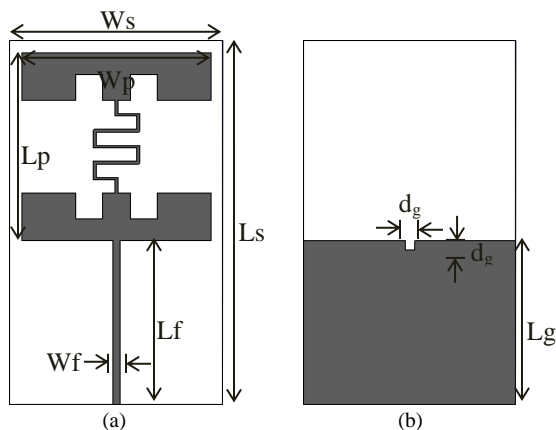


Fig. 13. Configuration of the double E-shaped meander line antenna with DGS (a) front view (b) back view.

### III. VARIOUS ANTENNA DESIGN TOPOLOGIES

The proposed double E-shaped meander line printed monopole antenna with DGS is built from several topologies as demonstrated by Fig. 15. The design process is started from a square printed monopole antenna which referred as a reference antenna. The square patch is then modified with the slots until the patch structure changes from square patch to I-shaped patch. Another slots are inserted onto the patch until it is modified from I-shaped patch to double E-shaped patch. The thin line that connects each of the E-shaped patch is then replaced by a meander line. Lastly, the DGS is introduced on the partial ground plane to improve the antenna reflection coefficient.

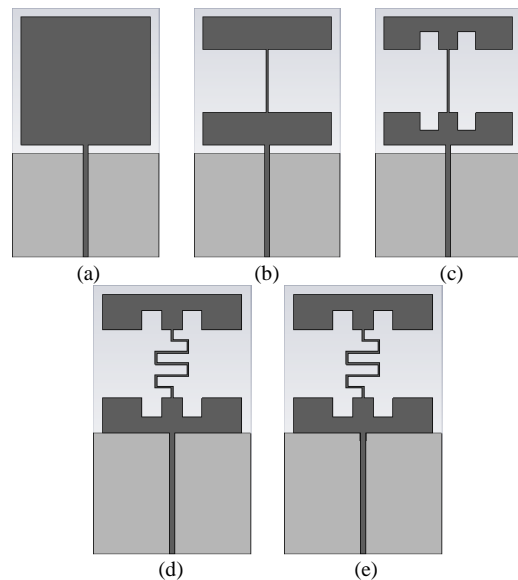


Fig. 15. Evolution of the (a) reference antenna (b) I-shaped antenna (c) double E-shaped antenna (d) double E-shaped meander line antenna (e) double E-shaped meander line antenna with DGS.

Fig. 16 displays the simulated reflection coefficient of various antenna topologies. The simulated reflection coefficient of the reference antenna is presented by the red

dash line with wideband behavior. The partial ground plane of the antenna produce wideband behavior and omnidirectional radiation pattern. The simulated reflection coefficient of the proposed antenna is presented by black solid line which resonates at 424 MHz. The proposed antenna produces narrow bandwidth characteristic due to the insertion of the slots and meander line. Eventhough the proposed antenna possess narrow bandwidth, it is not affecting the target applications since this antenna can be used for narrow band UHF applications where the size is more important.

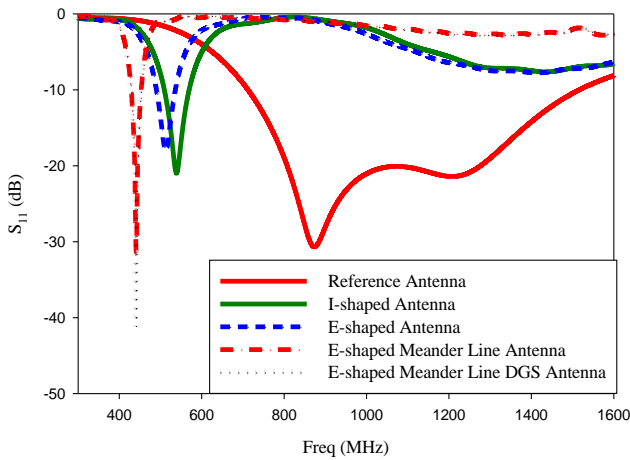


Fig. 16. Simulated reflection coefficient of various antenna topologies.

Better understanding on the antenna performances can be performed by studying the antenna current distributions. Antennas are divided into active and neutral zones [16]. Antenna active zone is the zone that the current is strongest on the antenna surface where geometry modifications would change the resonant frequency and impedance bandwidth. On the other hand, the neutral zone is where geometry modifications do not affect the antenna performances.

The insertion of the slots and meander line are based on the current distribution of the radiator. There are embedded on the patch where stongest current path is concentrated, hence the current on the radiator can be increased. Fig. 17 shows the surface current distribution of various antenna topologies.

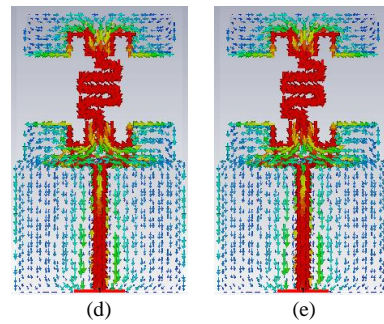
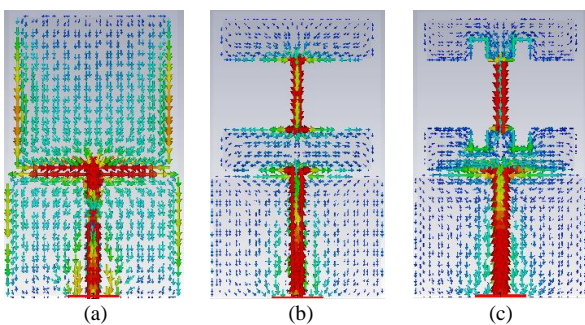


Fig. 17. Surface current distribution of the (a) reference antenna (b) I-shaped antenna (c) double E-shaped antenna (d) double E-shaped meander line antenna (e) double E-shaped meander line antenna with DGS.

All antennas that demonstrated previously radiate with omnidirectional radiation pattern. Simulated radiation pattern in the E-plane and H-plane for all antennas are demonstrated in Figure 18 and Figure 19, respectively. All antennas have similar omnidirectional radiation pattern in the E-plane and H-plane but with different amplitude due to the modification on the radiator.

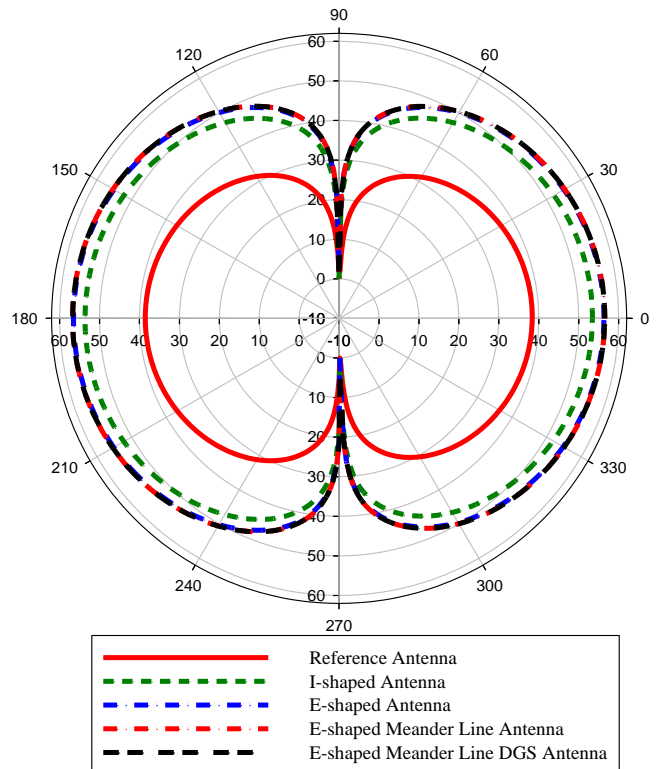


Fig. 18. Simulated E-plane Radiation Pattern for All Antenna Designs.

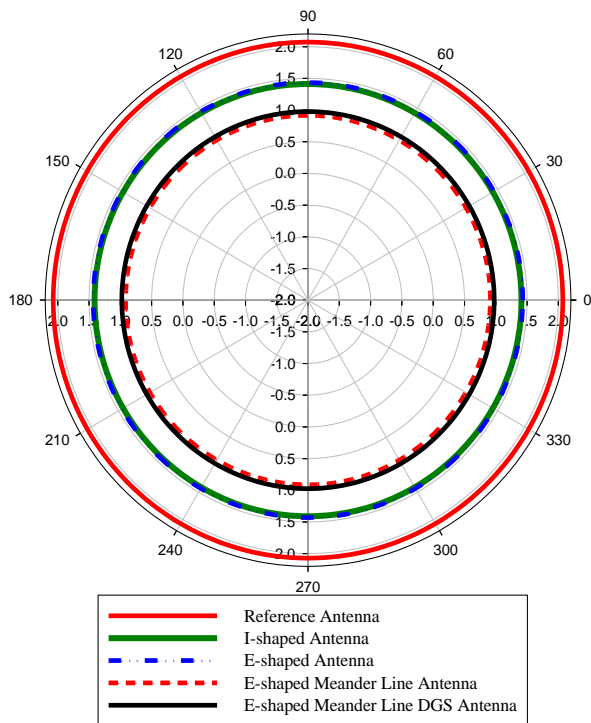


Fig. 19. Simulated H-plane Radiation Pattern for All Antenna Designs.

Summary of the performances of all antennas are depicted in Table I. For the reference antenna, its performance is taken only at resonant frequency of 878 MHz despite its wide bandwidth characteristics.

TABLE I  
PERFORMANCES OF ALL ANTENNAS

Antenna Type / Parameter	Freq. (MHz)	Return Loss (dB)	Gain (dBi)	Directivity (dB)	Efficiency (%)
Reference Antenna	878	-30.55	2.23	2.60	91.7
I-shaped Antenna	538	-20.94	1.55	2.01	89.2
Double E-shaped Antenna	512	-18.00	1.57	1.96	90.0
Double E-shaped Meander Line Antenna	442	-30.25	1.08	1.86	83.5
Double E-shaped Meander Line Antenna with DGS	440	-41.14	1.13	1.85	84.7

The performances of the proposed antenna has been compared with other antennas in literature as presented in Table II. The comparison is focusing on the size of the antenna, return loss, resonant frequency, antenna gain and antenna bandwidth. The size of the antenna is represented by the free space wavelength,  $\lambda_0$  since the resonant frequency of the antennas are vary. The proposed antenna exhibits better compromise between antenna size, gain and bandwidth

compared to other antennas in literature.

TABLE II  
COMPARISON RESULTS WITH OTHER ANTENNAS IN LITERATURE

References	Size	Frequency (GHz)	Gain (dBi)	Bandwidth (%)
Mitra, 2016 [1]	$0.139\lambda_0 \times 0.139\lambda_0$	1.90	-1.22	1.58
Ekke, 2017 [17]	$0.553\lambda_0 \times 0.569\lambda_0$	2.49	4.45	2.41
Wang, 2015 [18]	$0.033\lambda_0 \times 0.071\lambda_0$	0.433	-2.80	2.90
Gaetano, 2014 [19]	$0.074\lambda_0 \times 0.041\lambda_0$	0.433	-13	1.00
Liu, 2012 [20]	$0.074\lambda_0 \times 0.118\lambda_0$	0.433	-4.30	1.30
Liu, 2017 [21]	$0.068\lambda_0 \times 0.068\lambda_0$	2.4	-17	2.4
Proposed work, 2017	$0.123\lambda_0 \times 0.211\lambda_0$	0.440	1.13	5.64

#### IV. CONCLUSION

A novel double E-shaped meander line antenna with DGS on the partial ground plane has been designed, analyzed and investigated in this study. Parametric analysis has been conducted using GA optimizer to obtain the best parameters of the radiator. Combination of slots, meander line and DGS has reduces the antenna resonating frequency for about 436 MHz from 878 MHz to 440 MHz. Overall size of the proposed antenna is only 83.80 mm x 143.74 mm equivalent to  $0.123 \lambda_0 \times 0.211 \lambda_0$  where  $\lambda_0$  is a wavelength at 440 MHz. The proposed antenna possess an omnidirectional radiation pattern with adequate antenna gain of 1.13 dBi at UHF band.

#### ACKNOWLEDGMENT

The authors would like to thank Faculty of Electrical Engineering, Universiti Teknologi MARA. This work has been funded by Universiti Teknologi MARA under Holistic Success Module code no. 600-IRMI/DANA 5/3/ARAS (0028/2016).

#### REFERENCES

- [1] D. Mitra, B. Ghosh, A. Sarkhel, and S. R. B. Chaudhuri, "A Miniaturized Ring Slot Antenna Design With Enhanced Radiation Characteristics," *IEEE Trans. Antennas Propag.*, vol. 64, no. 1, pp. 300–305, 2016.
- [2] Z. Wang, Y. Yin, J. Wu, and R. Lian, "A Miniaturized CPW-Fed Antipodal Vivaldi Antenna with Enhanced Radiation Performance for Wideband Applications," *IEEE Antennas Wirel. Propag. Lett.*, vol. 15, pp. 16–19, 2016.
- [3] T. Fujimoto and R. Taniyama, "Miniaturization of a Printed Monopole Antenna for Circular Polarization," in *IEEE Antennas and Propagation Society, AP-S International Symposium (Digest)*, 2014, pp. 414–415.
- [4] S. Mondal, K. Mandal, and P. P. Sarkar, "Design of a shorted planar meander-line metal antenna," in *International Conference on Microelectronics, Computing and Communication, MicroCom 2016*, 2016, pp. 5–8.
- [5] R. K. Saraswat and M. Kumar, "Miniaturized Slotted Ground UWB Antenna Loaded With Metamaterial for WLAN and WiMAX Applications," *Prog. Electromagn. Res. B*, vol. 65, pp. 65–80, 2016.
- [6] R. Lian, Z. Wang, Y. Yin, J. Wu, and X. Song, "Design of a Low-Profile Dual-Polarized Stepped Slot Antenna Array for Base Station,"

- IEEE Antennas Wirel. Propag. Lett.*, vol. 15, pp. 362–365, 2016.
- [7] O. Caytan *et al.*, “Half-Mode Substrate-Integrated-Waveguide Cavity-Backed Slot Antenna on Cork Substrate,” *IEEE Antennas Wirel. Propag. Lett.*, vol. 15, pp. 162–165, 2016.
- [8] M. T. Ali, N. Ramli, M. K. M. Salleh, M. N. Tan, and S. Alam, “A Design of Reconfigurable Rectangular Microstrip Slot Patch Antennas,” pp. 111–115, 2011.
- [9] S. Yun and S. Nam, “Miniaturization of Cavity-Backed Crossed-Slot Antenna Using Folded Cavity,” pp. 155–156, 2013.
- [10] T. Sarkar, J. Chakravorty, and R. Ghatak, “Broadband Fractal Slot Planar Antenna,” no. 1, pp. 3–7, 2015.
- [11] A. A. N. Ovi, M. R. Chowdhury, M. R. A. Zuboraj, and M. A. Matin, “Design of Miniaturized Dual Band Microstrip Antenna Loaded With Asymmetric J Slot,” *J. Electr. Eng. Electron. Technol.*, vol. 2, no. 1, pp. 1–4, 2012.
- [12] V. Ghaffari, A. Tavakkoli, and R. M. Boroujeni, “Design Compact Planar Monopole Antenna for LTE Mobile Handset,” in *24th Iranian Conference on Electrical Engineering (ICEE)*, 2016, pp. 1244–1247.
- [13] C. A. Balanis, *Antenna Theory: Analysis and Design*. John Wiley & Sons, Inc., 2005.
- [14] M. Manohar, “Design, Fabrication and Testing of Printed Monopole Antennas for Super Wideband Applications,” Indian Institute and Electrical Engineering, 2014.
- [15] M. Sreejith, “Design and Development of Coplanar Strip Fed Planar Antennas,” Cochin University of Science and Technology, 2013.
- [16] D. Valderas, J. Legarda, I. Gutiérrez, and J. I. Sancho, “Design of UWB folded-plate monopole antennas based on TLM,” *IEEE Trans. Antennas Propag.*, vol. 54, no. 6, pp. 1676–1687, 2006.
- [17] V. Ekke and P. Zade, “Implementation of EBG Configuration for Asymmetric Microstrip Antenna to Improve Radiation Properties,” *J. Telecommun. Electron. Comput. Eng.*, vol. 9, no. 1, pp. 61–66, 2017.
- [18] X.-Y. Wang, Y. Fu, H. Wang, Y. Gui, and G.-M. Yang, “A Compact 433 MHz Antenna with Enhanced Performance by Using Multi-resonant Meander Line Structure,” in *Asia Pacific Microwave Conference*, 2015, pp. 1–3.
- [19] D. Gaetano, L. Loizou, J. Buckley, C. O’Mathuna, K. G. McCarthy, and B. O’Flynn, “Compact 433 MHz Antenna for Wireless Smart System Applications,” *Electron. Lett.*, vol. 50, no. 8, pp. 572–574, 2014.
- [20] W. Liu, Z. Zhang, and Z. Feng, “ISM 433-MHz Miniaturized Antenna Using the Shielding Box of Mobile Terminals,” *IEEE Antennas Wirel. Propag. Lett.*, vol. 11, pp. 330–333, 2012.
- [21] X. Liu, Z. Wu, Y. Fan, and M. Tentzeris, “A miniaturized CSRR loaded wide-beamwidth circularly polarized implantable antenna for subcutaneous real-time glucose monitoring,” *IEEE Antennas Wirel. Propag. Lett.*, vol. 16, pp. 577–580, 2017.



**Nabilah Ripin** received the Diploma in Electrical Engineering (Electronic) from Universiti Teknologi MARA, Dungun, Terengganu, Malaysia, in 2009 and the Bachelor Degree in Electrical Engineering (Communication), from Universiti Teknologi MARA, Shah Alam, Malaysia, in 2012. She is currently pursuing the PhD degree in

Electrical Engineering at UiTM, Shah Alam, Selangor, Malaysia.



**Ahmad Asari Sulaiman** is a senior lecturer in the Faculty of Electrical Engineering, Universiti Teknologi MARA (UiTM) Shah Alam, Selangor, Malaysia. He received his PhD in Microwave Engineering from Universiti Sains Malaysia (USM) in 2012. He was a Deputy Dean of Student Affairs from 2012 to 2016. His expertise been

accepted by other universities such as Anna University in

Chennai, India and Universiti Teknologi Petronas. He also led some national-level and universities research grants amounting more than RM 1.99 million.



**Nur Emileen Abd Rashid** is a senior lecturer in the Faculty of Electrical Engineering, Universiti Teknologi MARA (UiTM) Shah Alam, Selangor, Malaysia. She received her B.Eng in Electrical Engineering (Communications), from Universiti Kebangsaan Malaysia (UKM). She received her MSc in Telecommunications, Computer and Human Centred Engineering, from Universiti of Birmingham, UK. She received her PhD in Electrical Engineering (Radar Technology), from Universiti of Birmingham, UK in 2012.



**Mohamad Fahmi Hussin** is a senior lecturer in the Faculty of Electrical Engineering, Universiti Teknologi MARA (UiTM) Shah Alam, Selangor, Malaysia. He received his PhD in Engineering (Safety). Much of his work revolves around Safety (Policies, Management System, HIRARC). However, his passion also revolves around Electromagnetism. He has been awarded several research and community grants totaling to over RM 1.4 million (Graduate Employability, Exploratory Research Grant Scheme, Research Acculturate Grant Scheme).



**Nor Najwa Ismail** received the Diploma in Electrical Engineering (Electronic) from Universiti Teknologi MARA, Pulau Penang, Malaysia, in 2009 and the Bachelor degree in Electrical Engineering (Communication), from Universiti Teknologi MARA, Shah Alam, Malaysia, in 2012. She is currently pursuing the PhD degree in

Electrical Engineering at Universiti Teknologi MARA, Shah Alam, Malaysia.